INVESTIGATION OF THE THERMAL FATIGUE BEHAVIOUR OF

SINGLE-CRYSTAL NICKEL-BASED SUPERALLOYS SRR 99 AND CMSX-4

F. Meyer-Olbersleben [1], D. Goldschmidt [2] and F. Rézai-Aria [1]

1) Swiss Federal Institute of Technology MX-D
1015 Lausanne, Switzerland

2) MTU München GmbH - German Aerospace
8000 München, Germany

Abstract

Thermal fatigue (TF) behaviour in the low-modulus <001> direction of a new generation nickel-based single-crystal superalloy containing rhenium, CMSX-4 and a highly strengthened first generation one, SRR 99 is investigated. Both superalloys are subjected to comparative thermal fatigue testing. Thermal fatigue tests are performed on self-constraint single-edge wedge specimens. The transient mechanical strains within the thin edge tip of the TF specimens are measured and the anisothermal Manson-Coffin life curves are established. The effect of the maximum temperature, T_{max}, in the thermal cycles is evaluated from 1100 to 1175°C. Under identical test conditions a comparable crack propagation rate is observed for both single-crystal alloys. CMSX-4 has a good resistance to oxide-scale spalling. In CMSX-4 cracks initiate from small pores which have formed during solidification in interdendritic regions. In SRR 99, crater-like regions from where the crack can initiate, are formed by a mechanism of successive oxide-scale spalling and re-oxidation of the base alloy. The higher resistance of the oxide-scale in CMSX-4 to spalling combined with the higher strength of the corresponding γ' depleted zone improves its TF crack initiation resistance in comparison with SRR 99.

Superalloys 1992
Edited by S.D. Antolovich, R.W. Stusrud, R.A. MacKay,
D.L. Anton, T. Khan, R.D. Kissinger, D.L. Klarstrom
The Minerals, Metals & Materials Society, 1992

Introduction

The introduction of single-crystal (SX) superalloys has enhanced creep strength, oxidation resistance, temperature capability and turbine airfoil durability, relative to the earlier conventionally-cast equiaxed and directionally solidified (DS) columnar grain components. The main benefit of the SX-alloys is due to the fact that the natural direction of solidification <001> has the lowest Young modulus. Thus a substantial reduction has been achieved in the thermal stresses. These stresses arise from temperature gradients in the airfoil during start-up/shut-down operations or from gradients within the cooled airfoils. The materials developments, in particular DS and SX technologies, have allowed the loading of the vital components such as blades and vanes to be increased steadily. This has improved the turbine's efficiency and performance by increasing the gas turbine entry temperatures.

First generation SX-superalloys were cast with compositions slightly modified from those of nickel-base alloys used in conventional manufacture (1). Process and alloy development are now focused on the new generation SX-superalloys which are derivatives from the first generation. The main objective is the achievement of a high level of balanced mechanical properties (2) and oxidation resistance through the beneficial effects of adding rhenium and small quantities of yttrium. It is known that Re tends to concentrate in the γ-matrix, to stabilize the strengthening γ'-phase (3) and to alter γ/γ' misfit (4).

Extended research work has already been accomplished on the mechanical behaviour and properties of different SX-superalloys. However, these investigations concern mainly the creep and isothermal fatigue properties. Thermal fatigue (TF) behaviour of SX-superalloys, despite its key role, is less reported in the open literature. Laboratory TF tests on simple samples such as Glenny's tapered disc (5) and single (6, 7) or double-edge wedge specimens (8) have provided a realistic simulation of service conditions of polycrystalline real components. Nevertheless, there are no records of any measured transient thermal and mechanical strains in these specimens for polycrystalline as well as SX-alloys. For polycrystalline materials these parameters have been computed by finite elements method (FEM) using sophisticated heat transfer analysis combined with constitutive equations (9, 10, 11).

The validity of these equations has yet to be established by performing other isothermal simple tests (e.g. creep, fatigue, etc.) as well as anisothermal tests (e.g. thermo-mechanical fatigue, TMF). In TMF tests the behaviour of an element from a critical part (e.g. leading or trailing edge) of a real component is simulated using simple samples. Indeed, the temperature/strain/strain-rate (TSSR) histories to be simulated have first to be provided by means of FEM analysis of TF simple samples or real components. Moreover, due to testing limitations, the TMF cycle periods are generally long (i.e. low strain rate) in comparison with the real conditions. Furthermore, the constitutive equations taking into account the anisotropic mechanical behaviour of SX-alloys have yet to be developed. At present, the TSSR histories calculated for polycrystalline materials are used in TMF investigations of SX-alloys. Strain measurements on TF specimens have therefore became a main key for further assessments and understanding of the behaviour of the SX, DS as well as the polycrystalline alloys under conditions as near as possible to a real component in anisothermal loading. The strain measurements on simple samples such as single-edge wedge specimens will contribute to generate extended TSSR histories to be used in TMF investigations.

This study focuses on the investigation of the TF behaviour in the low-modulus <001> direction of a new generation nickel-based SX-superalloy containing rhenium, CMSX-4, and a highly strengthened first generation one, SRR 99. Both superalloys are subjected to comparative TF testing. Uncoated self-constraint single-edge wedge specimens are used. The transient mechanical strains within the TF specimens thin edge tip are measured and the anisothermal Manson-Coffin life curves are established. The effect of the maximum temperature, T_{max}, in thermal cycles is evaluated from 1100 to 1175°C.

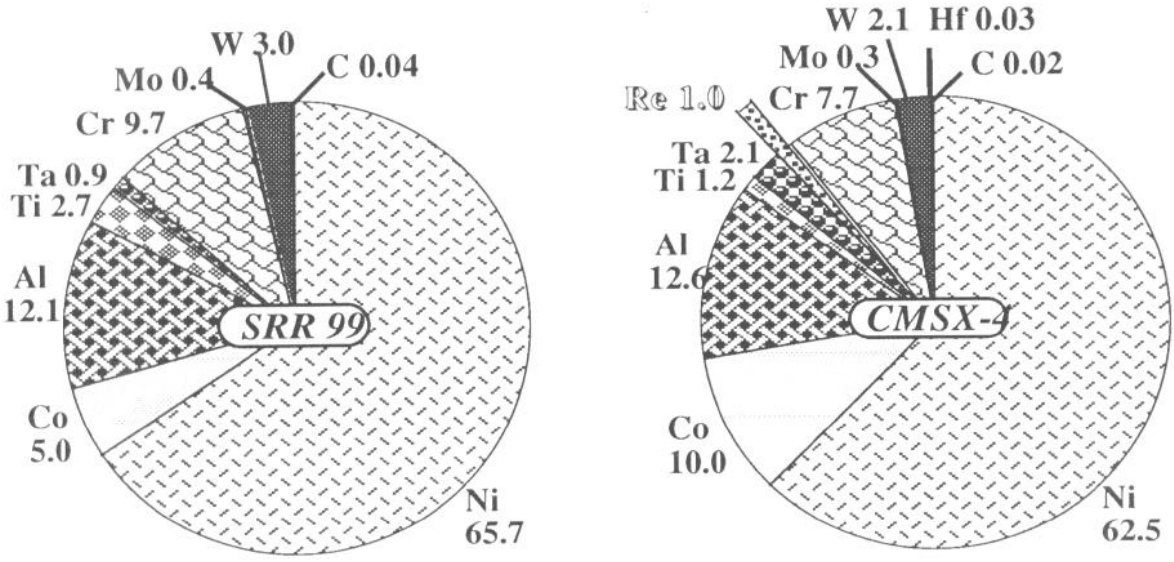

Figure 1 - Pie chart representation of atomic chemical composition (%).

Materials and experimental procedures

Materials

The chemical composition of both SX-superalloys are given in Figure 1 (atomic %). The two superalloys have a fully γ-solutioned structure with a regular cubic γ-morphology (Figure 2).

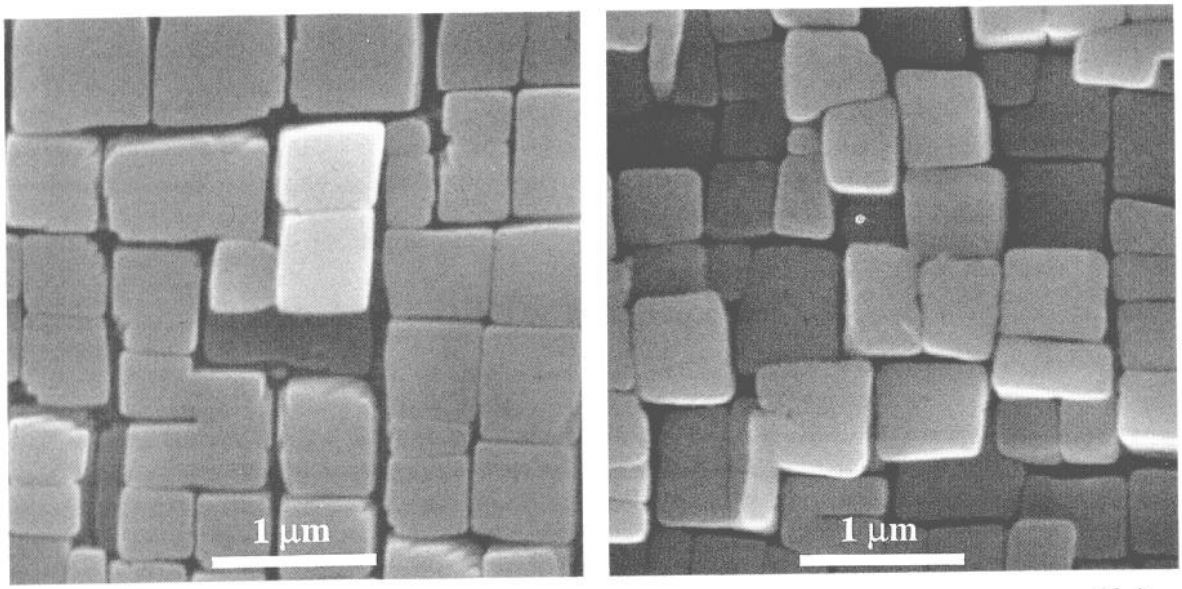

Figure 2 - Microstructure of CMSX-4(a) and SRR 99 (b).

Specimens preparation

The axi-symmetric specimens such as Glenny's disc or stepped disc (12) would not be convenient samples for TF investigations of SX-superalloys, due to the anisotropic mechanical behaviour of these alloys. The TF tests are carried out on self-constraint single-edge wedge specimens with edge radius (R) of 0.25 mm (6, 7). Their cross section is shown in Figure 3. The specimens are first cut by electro-discharging machining (EDM) from cast slabs and then machined such that the angle between the low-modulus <001> direction and the longitudinal axis is less than 6°. Care is taken to avoid the induced residual stresses in the thin edge tip during specimens preparation. All the specimens are mechanically polished parallel to the longitudinal axis by diamond pastes down to 1 µm.

TF procedure

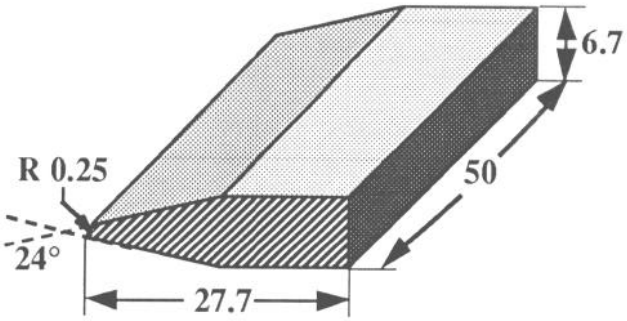

Figure 3 - Schematic presentation of self-constraint single-edge wedge TF specimens (all dimensions in mm).

A new TF rig using induction heating is developed (Figure 4). The TF specimen, placed on three vertical Silica rods, is totally free to expand and contract during heating and cooling. The thermal strain and subsequent thermal stress are induced in the specimen only by the difference on thermal expansion through the specimen. The edge of the specimen is in a horizontal plane and the specimen is uniformly heated and cooled along the thin edge. Induction heating is provided via a Hüttinger solid-state 6.0 kW (200 kHz) high frequency generator coupled to a special coil and driven by a programmable temperature controller (Eurotherm model 818 P). Air cooling is provided via a copper nozzle placed in front of the edge. A Chromel-Alumel thermocouple (ø 0.1 mm) spot-welded at 2.5 mm from the edge monitors the test using a pre-calibrated chart of temperature distribution on the surface. The TF rig is very flexible and can perform numerous very rapid TF cycles.

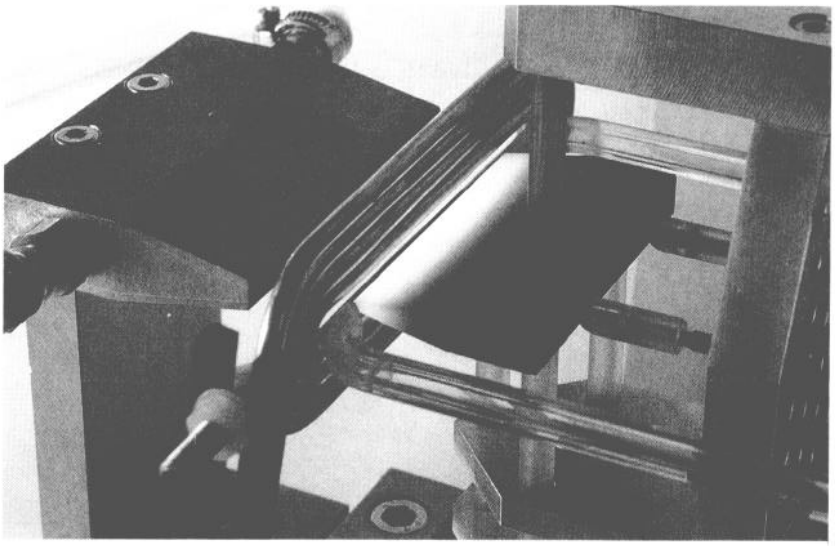

Figure - 4 Thermal fatigue rig.

In the first step, the temperature gradient along the edge of one dummy specimen is determined in order to ensure a uniform heating and cooling along the specimens longitudinal axis. The thermocouples are spot-welded on the edge and at 2.5 mm from it on the wedge surface. A pyrometer (Quotienten-Pyrometer Maurer) is used to check the temperature measurements by thermocouples. It was observed that the measured temperatures depend upon the diameter of the thermocouple used. The smaller the thermocouple diameter the more accurate the temperature obtained. The thermocouple ø 0.1 mm gave the measured temperature nearest to the pyrometer response. Tests are performed at T_{max} varying from 1100°C to 1175°C with T_{min} being maintained constant at 200°C throughout the test series. The heating and cooling period are respectively 60 and 20 s. The tests are interrupted at regular intervals to investigate the crack initiation and propagation. After completion of tests the cross sections parallel to the thin edge are examined by Scanning Electron Microscopy (SEM) and optical microscopy.

TF strain measurements procedure

A special extensometer system is developed in order to measure the mechanical strain within the edge tip. The two quartz-arms of the extensometer are placed at 2R mm from the edge on the two end surfaces of the specimens which are perpendicular to the longitudinal axis (Figure 4). The total mechanical strain, ε_m, is defined as the difference between the total measured strain, ε_{tot}, and the free thermal dilatation, ε_{th} ($= \alpha \times \Delta T$ where $\Delta T = T - RT$). Temperature (T) is also measured on the wedge surface at 2R mm from the edge. The edge

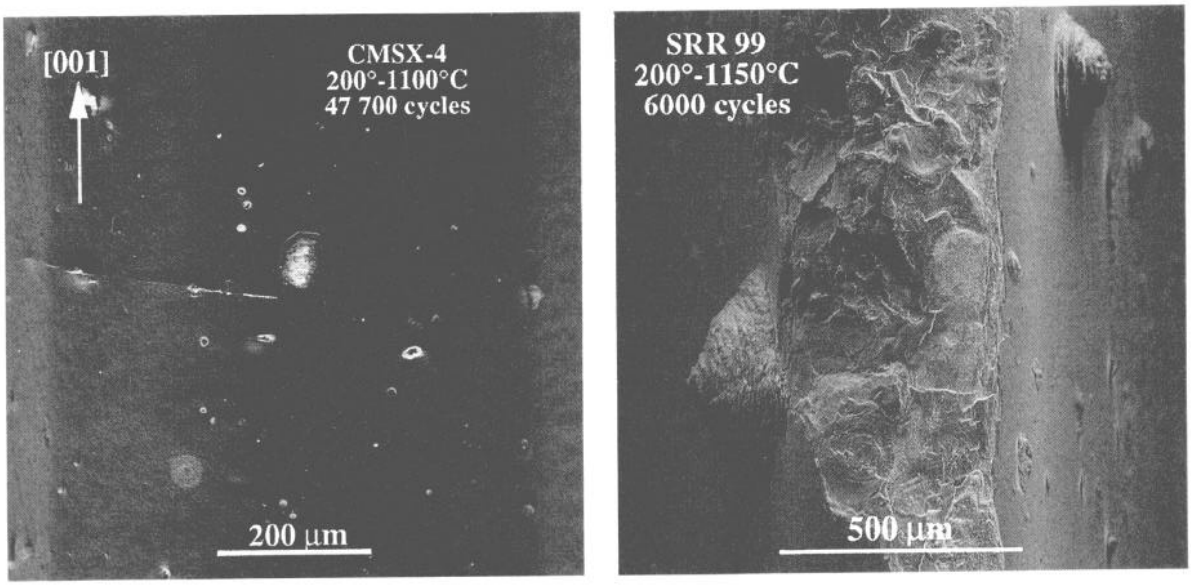

Figure 5 - Direct frontal view of the edge tip of TF specimens after TF cycling. Note the crack initiation from a small pore in CMSX-4.

tip is considered as a cylinder which is uniformly heated/cooled along its longitudinal axis. The temperature distribution analysis by FEM has shown that this hypothesis is satisfied. The "out-of-plane" total displacements at any point within these two surfaces can be measured by this system and used as boundary conditions in FEM analysis (13).

Results and discussion

TF crack initiation mechanisms and microscopic observations

During TF testing it was noted that CMSX-4 provides better oxide-scale adherence than SRR 99. The CMSX-4 specimens remain relatively intact during TF cycling while the edges of the SRR 99 specimens, because of high oxide-scale spalling, are severely damaged (Figure 5). In CMSX-4, cracks initiate from small oxidized pores on the edge surface (Figure 5). These pores are formed during solidification in the interdendritic regions. By a mechanism of oxide-scale spalling and re-oxidation of the base alloy, highly oxidized crater-like regions are formed on SRR 99 specimens from where cracks could initiate (14). The small oxidized pores on the edge surface are also the preferable sites for the formation of such crater-like regions. However, not necessarily all the small pores contribute to the formation of these regions. Observations on the cross section have revealed a compact oxide and oxide/metal interface in CMSX-4 (Figure 6). The oxide-scale in CMSX-4 is about two times thinner than in SRR 99. In SRR 99 the pores are abundantly present within the oxide-scale and at the oxide/metal interface which suggests its poor mechanical properties under TF loading.

As generally observed in creep tests of SX-superalloys, the microstrucutre evolves under TF cycling (15, 16). Figure 6 shows the evolution of the well-defined γ'-cubic precipitates of both SX-alloys to a rafted or globular morphology. The shape and dimensions of the γ' precipitates change from the edge tip to the core of the specimens due to the changes in thermal strains and temperature. However, this microstructural modification is less pronounced in CMSX-4 as compared to SRR 99, due probably to a positive effect of Re addition (4).

TF crack growth

Figure 7 shows the evolution of the longest cracks for different T_{max}. In both SX-alloys, cracks initiate after a few thousand thermal cycles. Corresponding TF crack propagation rates (TFCPR) are plotted vs the square root of crack length ($\sqrt{a}$) in Figure 8. Despite the absence

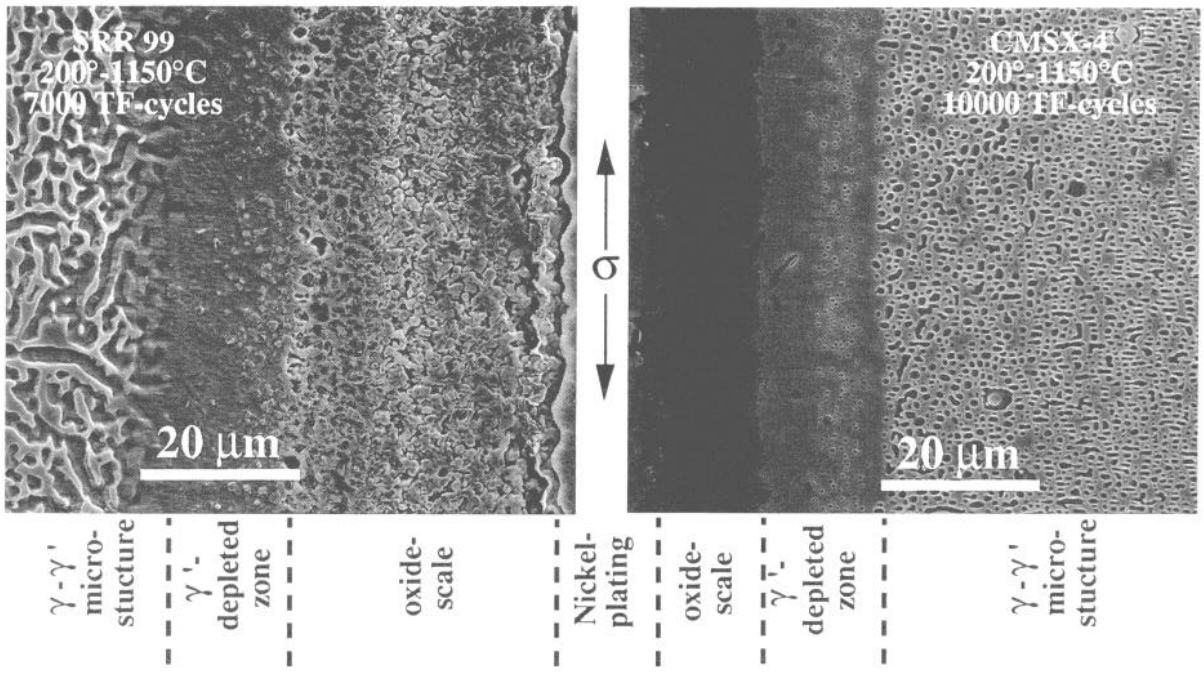

Figure 6 - Microstructures at thin edge tip of both superalloys after thermal cycling.

of stress intensity factor calculations for the TF specimens used, it is known from LEFM that ΔK_I is proportional to $\sqrt{a}$. As T_{min} has been maintained constant throughout the tests, a higher T_{max} induces a higher TF loading and, consequently, a higher TFCGR, at least for short cracks. The higher TF crack growth resistance as the crack propagates inside the specimen can be explained basically by the fact that the thermal gradient and corresponding thermal loading decrease inwards from the edge. Mowbray et al. (17) have calculated the ΔK_I expression for the Glenny's tapered disc specimen. They have, at least qualitatively, shown that ΔK_I increases with increasing crack length until a relatively constant value and then decreases at longer crack length. Therefore, as the crack propagation driving forces are reduced inside the specimen, TFCGR decreses too. Under identical test conditions the two SX-alloys as well as an Yttrium-modified CMSX-4+Y (14) show roughly the same crack propagation resistance. Thus, the modifications in composition, in particular the addition of Re and Y, do not dramatically improve the TF propagation resistance of CMSX-4 in

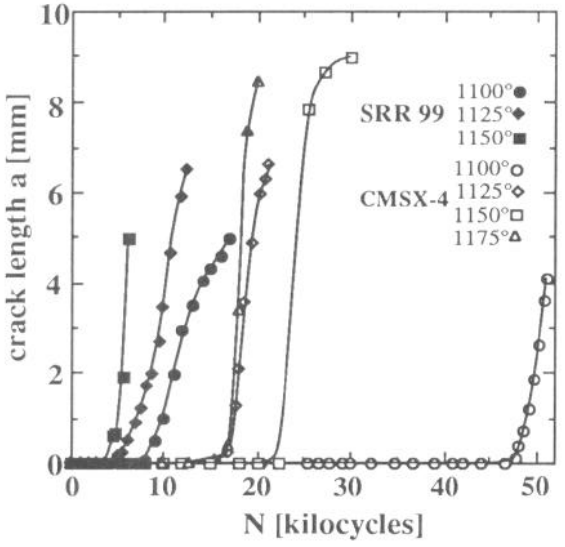

Figure 7 - Evolution of the longest crack a vs TF cycles.

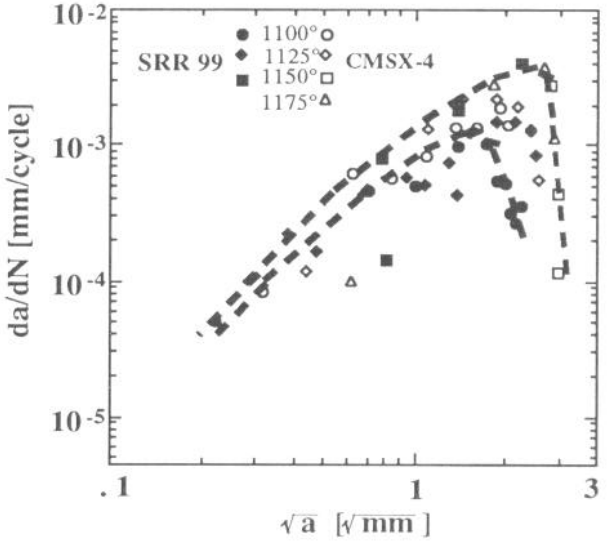

Figure 8 - TF crack propagation rate vs square root of the crack length.

comparison to SRR 99.

Strain measurements and anisothermal Manson-Coffin life curves

As mentioned in the introduction, strain measurements during TF loading are very important. The anisothermal Manson-Coffin life curves, for example, can be obtained under conditions very near to a real component loading. Moreover, the TF resistance of the materials are generally investigated on the basis of a "standard-in-house thermal cycle" reporting TFCIL vs T_{max}. From a strict scientific and engineering point of view the most important parameter is obviously the mechanical strain and not temperature per se. Furthermore, the absence of strain measurements may explain the differences in TF investigations results. Therefore, strain measurements would contribute to overcome this major limitation of the TF simple specimens.

An example of the variation of measured total transient strain (ε_{tot}) vs measured temperature at the thin edge tip is reported in Figure 9 and compared to the free thermal dilatation, ε_{th}. The variation of the corresponding mechanical strain ($\varepsilon_m = \varepsilon_{tot} - \varepsilon_{th}$) vs temperature is reported in Figure 10. These curves correspond to a stabilized thermal cycle. As shown in Figure 10, the presumed cylinder at the edge tip is put under compressive straining during heating, reaching its maximum values (ε_m^{min}) at T_{max}. In cooling, the cylinder goes rapidly into tension up to a maximum strain within a few seconds and then decreases to a residual tensile strain at T_{min}. During cooling the maximum strains (ε_m^{max}) are always observed at intermediate temperature.

The ε_{tot} - T curve (Figure 9) helps to better understand the ε_m - T curve. Imagine that the assumed cylinder is detached from the rest of the specimen and put under the same thermal cycle. At each temperature, it would have a free thermal dilatation equal to ε_{th}. However, during TF cycling a non-uniform thermal expansion is produced within the specimen, hindering the free dilatation of the cylinder. The measured total strain ε_{tot} is thus this hindered expansion. The difference between ε_{tot} and ε_{th} leads to a mechanical straining which has a thermal (and not mechanical) origin.

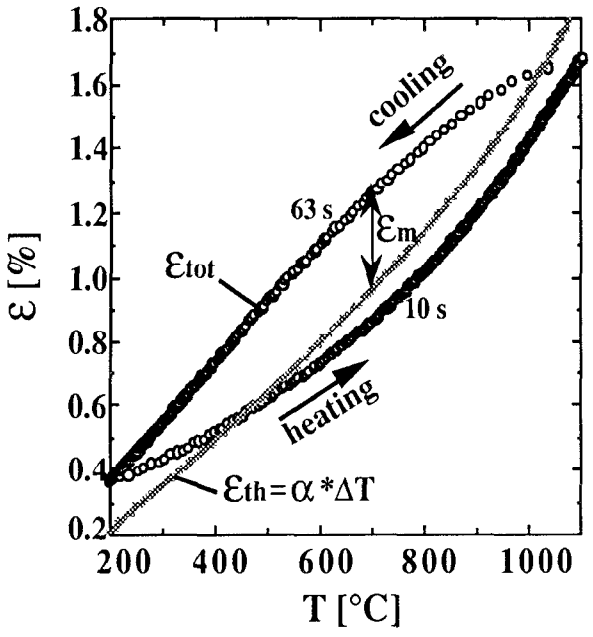

Figure 9 - Variation of measured total strain with measured temperature at the edge tip of a TF specimen.

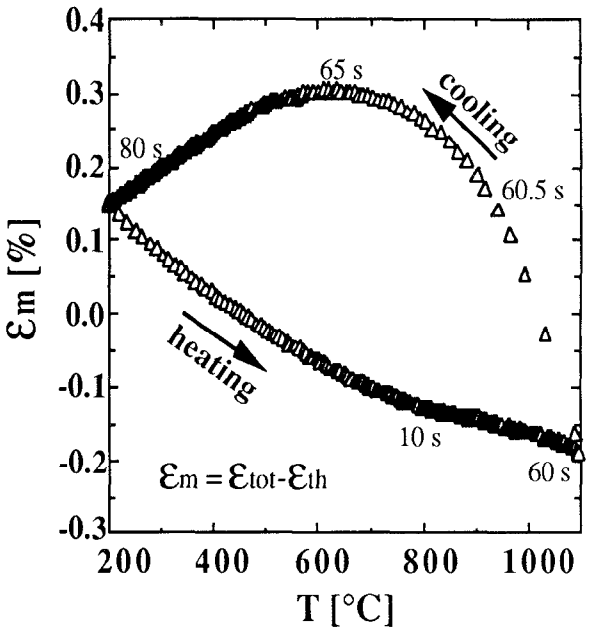

Figure 10 - Variation of measured mechanical strain with measured temperature at the edge tip of a TF specimen.

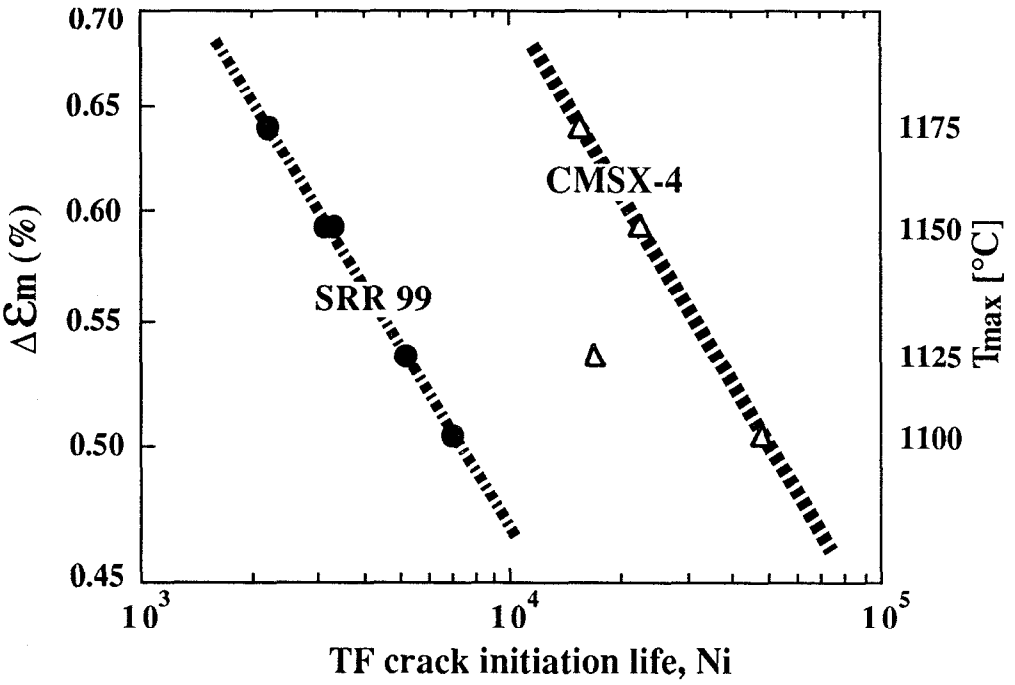

Figure 11 - Variation of TF crack initiation life N_i, as a function of T_{max}.

TF crack initiation life (TFCIL), defined as the number of thermal cycles required to form a principal crack of 0.1 mm length, is plotted in Figure 11 vs the mechanical strain range, $\Delta\varepsilon_m$ ($\varepsilon_m^{max} - \varepsilon_m^{min}$), for both SX-superalloys. By decreasing T_{max}, $\Delta\varepsilon_m$ decreases at the edge and thus TFCIL increases for both alloys. At any $\Delta\varepsilon_m$, CMSX-4 has a better TFCIL than SRR 99.

Under the investigated TF testing conditions the crack propagation resistance of both superalloys as well as CMSX-4+Y (14) were roughly identical, despite the different γ' morphology changes observed. It has already been reported that isothermal crack propagation resistance of SRR 99 was not altered by γ' morphology (18). For the SX-alloys studied, the TFCIL constitute about 70 to 90% of the total TF life (defined as the number of thermal cycles required to form a principal crack of 1 mm length). For polycrystalline nickel- (7) and cobalt-based (6) superalloys the TFCIL is generally less than 50% of the total life. Thus more attention has to be focused on the crack initiation of SX-superalloys subjected to TF loading.

During thermal cycling and prior to any crack propagation, a "composite-like" layer forms on the surface at the thin edge. This "composite" consists of an oxide-scale and its corresponding γ' depleted zone (DZ). The oxide-scale possesses complicated chemical and mechanical properties and is generally more brittle than the neighbouring γ' DZ. A higher strength DZ would enhance the resistance of the "composite", i.e. the critical stress to fracture of a representative element of the material, and thus enhance the TFCIL. A set of tests, performed at T_{max} = 1150°C on SRR 99, have shown that the microhardness within the γ' DZ decreases continuously with increasing TF cycles (19).

The relative Vickers microhardness (RHv) is defined as the ratio between the γ' DZ microhardness and the virgin material microhardness. As an example, the RHv is reported vs the number of TF cycles at the end of tests performed at T_{max} = 1150°C, for CMSX-6 (16), SRR 99 (19) and CMSX-4 (Figure 12). As shown in Figure 12, the DZ of CMSX-4, which has the best TFCIL, looses only about 3% of its virgin microhardness following 30000 TF cycles while SRR 99 and CMSX-6 (the lowest TFCIL) looses respectively about 10% (7000 cycles) and 26% (4000 cycles). The higher TFCIL of CMSX-4 would thus be explained by the higher resistance of its oxide-scale to spalling combined with the higher strength of the corresponding γ' depleted zone, due presumably to the higher γ' precipitates stability within the DZ.

Summary and conclusions

The TF behaviour of the low-modulus <001> direction of a SX nickel-based superalloy containing rhenium, CMSX-4, is investigated and compared with the TF resistance of SRR 99. A significant enhancement of TF crack propagation resistance by Re-addition has not been observed. However, the higher oxidation resistance of CMSX-4 combined with its higher γ'-phase stability improves its TFCIL in comparison with SRR 99. In CMSX-4, cracks initiate from small pores. In SRR 99, crater-like regions are formed by a mechanism of successive oxide-scale spalling and re-oxidation of the base metal during TF. These regions are prone to crack initiation. The early and new generation SX-superalloys provide a significant progress in TF durability and temperature capability in comparison to the polycrystalline as-cast superalloys (Figure 14). SX-superalloys provide also a lower TFCGR as compared to polycrystalline alloys.

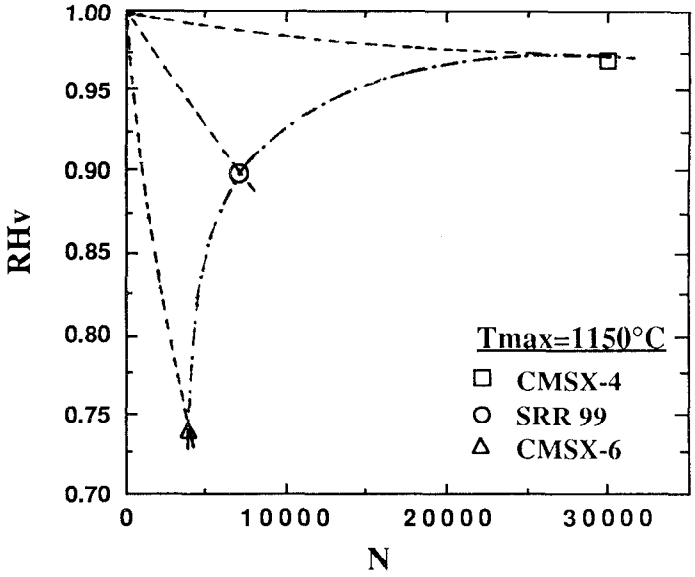

Figure 12 - Variation of the relative microhardness of the γ' DZ vs of number of TF cycles.

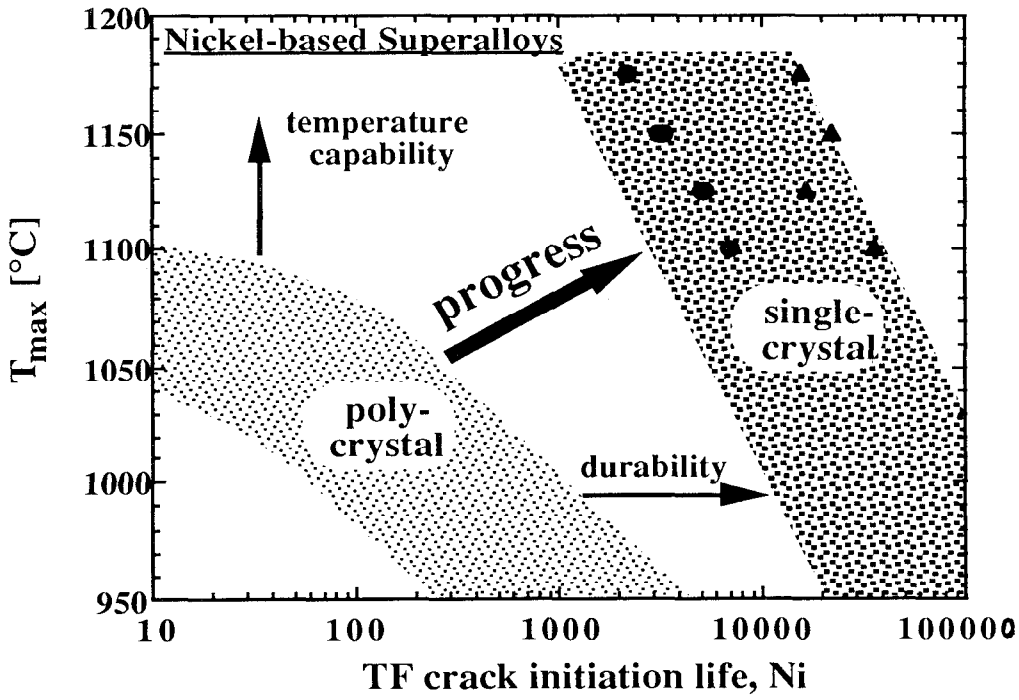

Figure 13 - Progress in durability and temperature capability of as-cast nickel-based superalloys from polycrystalline [IN 100 (7)] to single crystalline.

Acknowledgment

The authors would like to thank Prof. B. Ilschner for his helpful discussions, and the COST 501-2 research program for the financial support.

References

1. K. Harris, G. L. Erickson and R. E.Schwer, "Development of the CMSX* series of single crystal alloys for advanced technology turbine components", Novel techniques in metal deformation testing, ed. R. H. Wagoner (Warrendale - Pa. : Metall. Society of AIME, 1983).

2. K. Harris, G. L. Erickson and R. E. Schwer, "CMSX single crystal, CM DS & integral wheel alloys properties & performance", High Temperature Alloys for Gas Turbines and Other Applications 1986, ed. W. Betz et al. (Dordrecht : Kluwer, 1986), 709-728.

3. S. M. Foster, T. A. Nielsen and P. Nagy, "Enhanced rupture properties in advanced single crystal alloys", Superalloys 1988, ed. D. N. Duhl et al. (Warrendale-Pa:TMS, 1988), 245-254.

4. A. F. Giamei and D. L. Anton, "Rhenium additions to a Ni-base superalloy : effects on microstructure", Metallurgical Transactions A, 16A (1985), 1997-2005.

5. E. Glenny, "The influence of specimen geometry on thermal fatigue behaviour", Thermal and high strain fatigue, (London:The Inst. of Metals &The Iron and Steel Inst.,1967),346-363.

6. F. Rézai-Aria, M. François and L. Rémy, "Thermal fatigue of MAR-M509 superalloy - I. The influence of specimen geometry", Fatigue Fract. Eng. Mater. Struct., 11 (1988), 277-289.

7. F. Meyer-Olbersleben, "Mechanische und Mikrostrukturelle Untersuchungen zur Thermischen Ermüdung von IN 100" (Diplomarbeit, Universität Erlangen-Nürnberg und Swiss Federal Institute of Technology, Lausanne, Switzerland 1990).

8. M. A. H. Howes, "Thermal fatigue data on 15 Nickel- and Cobalt-base alloys" (NASA CR-72738, National Aeronautics and Space Administration, May 1970).

9. D. F. Mowbray and J. E. McConnelee, "Nonlinear analysis of a tapered disc thermal fatigue specimen", Thermal Fatigue of Materials and Components, ASTM-STP 612, ed. D. A. Spera and D. F. Mowbray (Philadelphia - Pa : ASTM, 1976), 10-29.

10. F. Rézai-Aria, B. Dambrine and L. Rémy, "Thermal fatigue of MAR-M509 superalloy - II. Evaluation of life prediction models", Fatigue Fract. Eng. Mater. Struct., 11 (1988), 291-302.

11. A.L. Ramteke, F. Meyer-Olbersleben and F. Rézai-Aria,"Three dimensional thermal strain and stress analysis of single-edge wedge specimens" (accepted to be presented at the 3rd Int. Conf. on Low Cycle Fatigue and Elasto-Plastic Behaviour of Materials, LCF3, Berlin, 7-11 September 1992).

12. J. W. Holmes, F. A. McClintock, K. S. O'Hara and M. E. Conners, "Thermal fatigue testing of coated monocrystalline superalloys", Low Cycle Fatigue, ASTM-STP 942, ed. H. D. Solomon et al. (Philadelphia - Pa : ASTM, 1988), 672-691.

13. To be published.

14. S. Draper, D. Hull and R. Dreshfield, "Observations of directional gamma prime coarsening during engine operation", Metallurgical Transactions A, 20A (1989), 683-688.

15. F. Meyer-Olbersleben et al., "Thermal fatigue of an yttrium-modified single-crystal superalloy" (accepted to be presented at the 3rd Int. Conf. on Low Cycle Fatigue and Elasto-Plastic Behaviour of Materials, LCF3, Berlin, 7-11 Sept. 1992)

16. C. Jaquerod,"Changement structural en fatigue thermique d'un superalliage monocristallin à base Ni, CMSX-6" (scientific training report, Swiss Federal Institute of Technology, 1991).

17. D. F. Mowbray, D. A. Woodford and D. E. Brandt, "Thermal fatigue characterization of cast cobalt and nickel-base superalloys", Fatigue at Elevated Temperature, ASTM-STP 520, ed. A. E. Carden, A. J. McEvily and C. H. Wells (Philadelphia - Pa : ASTM, 1973), 416.426.

18. M.B. Henderson and J.W. Martin,"The effect of gamma-prime phase distribution on elevated temperature fatigue crack propagation in a single crystal superalloy", High temperature materials for power engineering 1990, ed. E. Bachelet et al. (Dordrecht:Kluwer,1990),987-996

19. C. M. Engler-Pinto, "Thermal fatigue tests and microstructure analysis of a nickel-based single-crystal superalloy, SRR 99" (scientific training report, in portuguese, University of Campinas-SP and Swiss Federal Institute of Technology, Lausanne, Switzerland, 1992).